Korean J. Chem. Eng., 35(4), 819-825 (2018)
DOI: 10.1007/s11814-017-0329-1

pISSN: 0256-1115
eISSN: 1975-7220

Fuzzy-based nonlinear PID controller and its application to CSTR

Gun-Baek So* and Gang-Gyoo Jin,†**

*Department of Convergence Study on the OST, Korea Maritime and Ocean University,
727 Taejongro, Yeongdo-gu, Busan 49112, Korea
**Division of IT, Korea Maritime and Ocean University, 727 Taejongro, Yeongdo-gu, Busan 49112, Korea
(*Received 26 July, 2017 • accepted 23 November, 2017*)

Abstract−This study presents a new design method for a nonlinear variable-gain PID controller, the gains of which are described by a set of fuzzy rules. User-defined parameters are tuned using a genetic algorithm by minimizing the integral of absolute error and the weighted control input deviation index. It was observed in the experimental results on a continuous stirred tank reactor (CSTR) that the proposed controller provided performances: overshoot $M_p \leq 1.25\%$, 2% settling time $t_s \leq 1.71$ s and IAE≤1.26 for set-point tracking, perturbance peak $M_{peak} \leq 0.05\%$, 2% recovery time $t_{rcy} \leq 3.97$ s and IAE≤0.10 for disturbance rejection, and $M_{peak} \leq 0.04\%$, $t_{rcy} \leq 2.74$ s and IAE≤0.04 for parameter changes. Comparison with those of two other methods revealed that the proposed controller not only led to less overshoot and shorter settling time for set-point tracking and less perturbance peak and shorter recovery time for disturbance rejection, but also showed less sensitivity to parameter changes.

Keywords: PID Controller, Nonlinear Gains, Tagaki-Sugeno Fuzzy Rule, Continuous Stirred Tank Reactor (CSTR)

INTRODUCTION

Most processes in process industries show time-varying and high nonlinearity characteristics. In particular, a continuous stirred tank reactor (CSTR) operated in petrochemical plants is significantly affected by the concentration, temperature, pressure, catalyst, and residence time, and it needs to be operated near an unstable equilibrium point for a long time in some cases [1-3]. One of the most common controllers that have been extensively used in process industries is the proportional-integral-derivative (PID) controller. The PID controller has survived many changes in technology, from mechanics and pneumatics to microprocessors, because of its simplicity of structure and parameter tuning, high reliability, and cost-effectiveness. Linear fixed-gain PID controllers can be expected to perform satisfactorily as long as the process is operated in a range sufficiently close to a nominal operating point. They cannot guarantee a good control performance with changes in operating points or environmental circumstances. To solve this problem, many research efforts have been made to incorporate intelligent features, such as automatic tuning, sliding mode control, adaptation, neural networks, fuzzy theory, and evolutionary algorithms [4-12]. Recently, nonlinear control tools have been introduced in the design of PID controllers [13-20].

Among many approaches, nonlinear PID (NPID) control is viewed as one of the most effective and simple methods. Recently, novel approaches have been studied to design NPID controllers that introduce several types of nonlinear elements to the frame of the standard PID controller to provide a more precise and stable performance. NPID controllers have been known to alleviate some control problems occurring in linear PID controllers by largely employing nonlinear elements in the PID control scheme. NPID controllers come in various forms depending on the control objective and application strategy, as implied by the term *nonlinear*. Recent approaches for applying nonlinear elements to the PID control scheme can be divided into two broad classes: to adopt a nonlinear gain in cascade with a linear fixed-gain PID control architecture to scale the error between the set-point and the actual output [13-15], and to adopt time-varying controller gains that are a nonlinear function of the error and/or error rate [16-20].

Studies have been conducted with the former approach. Seraji [13] introduced a new class of NPID controllers that comprise a sector-bounded nonlinear gain in cascade with a linear fixed-gain P, PD, PI, or PID controller. Sigmoid, hyperbolic, and piecewise-linear functions are proposed for the nonlinear gain. Su et al. [14] suggested a method in which an error is multiplied by the sector-bounded function of the error and is entered into a standard PID controller, the gains of the controller are tuned using the Ziegler-Nichols method, and it is applied to a two-degree-of-freedom robot arm. Li et al. [15] proposed an anti-windup compensator scheme based on a nonlinear tracking differentiator and nonlinear combination and used it for improving the wing control performance of a missile. Conversely, studies have also been made with the latter approach. Zhang and Hu [16] proposed a standard PID controller with three gains using the hyperbolic secant and exponential functions for error and applied it to the excitation control system of a generator. Korkmaz et al. [17] suggested three nonlinear gains that are characterized by the Gaussian error function and suggested a method for tuning the parameters using a genetic algorithm (GA). Chen et al. [18] proposed an NPID control for an electro-hydraulic servo system in which three gains are adjusted by a series of non-

†To whom correspondence should be addressed.
E-mail: ggjin@kmou.ac.kr

linear functions and the error. Lucas et al. [19] proposed an adaptive PID control based on gaussian functions, which are functions that present predefined higher and lower limits. Mishra et al. [20] proposed a nonlinear PI Controller which inherits from a classical PI control structure with the varying-integral gain in accordance with the error and error rate. All these methods have shown satisfactory results in different control environments, but further improvements are needed.

This study presents a nonlinear PID controller with tuning gain values that are continuously changed while the process is in operation. To overcome the limitation of an ideal derivative action, a practical derivative term with a first-order filter is used and an input saturation commonly used in industrial sites is considered. The parameters of nonlinear proportional, integral, and derivative gains are a set of fuzzy rules of the Tagaki-Sugeno form tuned using a GA in terms of minimizing the integral of absolute error and weighted control input deviation performance index. The proposed method is applied to the temperature control of a CSTR process to demonstrate set-point tracking and disturbance rejection performances and robustness to parameter changes.

CONTINUOUS STIRRED TANK REACTOR (CSTR)

CSTRs are known to be difficult to analyze or control because of their complex behavior [5]. Let us consider a CSTR in which an exothermic, first-order reaction A→B takes place. Fig. 1 depicts its schematic diagram. To maintain an optimal condition in which a perfect reaction occurs within the reactor, the internal temperature needs to be maintained constant along with strong agitation. C_f, T_f, F_f and C, T, F denote the concentration [mol/m^3], temperature [K], and flow [m^3/sec] at the inlet and outlet of the reactant, respectively. T_{cf}, F_{cf} and T_c, F_c are the temperature and flow at the inlet and outlet of cooling water, respectively.

The mathematical model is given by [1,2,5]

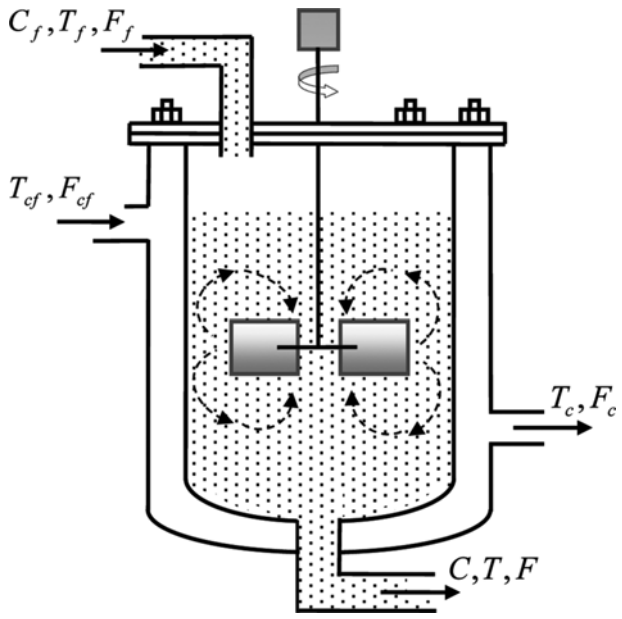

Fig. 1. Non-isothermal CSTR proces.

$$\dot{x}_1 = -x_1 + D_a(1-x_1)\exp\left(\frac{x_2}{1+x_2/\gamma}\right) + d_1, \tag{1a}$$

$$\dot{x}_2 = -(1+\beta)x_2 + HD_a(1-x_1)\exp\left(\frac{x_2}{1+x_2/\gamma}\right) + \beta u + d_2, \tag{1b}$$

$$y = x_2, \tag{1c}$$

where x_1 and x_2 are the dimensioness concentration C and temperature T, respectively; y and u the outlet temperature of the product and the temperature of cooling water, respectively; d_1 and d_2 disturbances; D_a the Damköhler number; H the heat of reaction; β the heat transfer coefficient; V the volume of CSTR [m^3]; γ=E/R T_f, E activation energy [cal/mol]; and R the gas constant [cal/mol-K]. The open-loop system in Eq. (1) has nominal values D_a=0.072, γ=20, H=8, and β=0.3 [5]. x_1, x_2, u, and t are dimensionless variables as

$$x_1 = \frac{C_f - C}{C_f},\ x_2 = \frac{T - T_f}{T_f}\gamma,\ u = \frac{T_c - T_f}{T_f}\gamma,\ t = t'\frac{F_f}{V}. \tag{2}$$

As the flow-changing valve operates in a physical limited range of input signals, that is, between fully open and fully closed, we implement effective control under a saturation function defined by

$$\mathrm{sat}(u) = \begin{cases} u_{min} & \text{if } u < u_{min} \\ u & \text{if } u_{min} \le u \le u_{max} \\ u_{max} & \text{if } u > u_{max} \end{cases}, \tag{3}$$

where u_{min}=−5 and u_{max}=5. Therefore, u_{sat}=sat(u).

CONTROLLER DESIGN

1. Structure of the Proposed NPID Controller

To mitigate an undesirable effect called *derivative kick* that can occur in a standard PID controller because of a noisy sensor or a small sampling time, an NPID controller with a first-order filter added to the derivative term is proposed in this work.

$$C(s) = K_p(e) + \frac{K_i(e)}{s} + \frac{K_d(e,\dot{e})s}{1+T_f(e,\dot{e})s}, \tag{4}$$

where three gains K_p(e), K_i(e), and K_d(e, ė) are time-varying nonlinear functions of the error e and error rate ė. They have the same meanings as K_p, K_i and K_d in the standard PID controller. The last term in (3) denotes the approximate derivative, where T_f(e, ė)=T_d (e, ė)/N and T_d (e, ė)=K_d (e, ė)/K_p(e). N is a fixed value that is empirically determined between 8 and 20 [21,22]. N=10 is used in this study because the change in N does not affect significantly the optimal values of other tuning parameters in our simulation works.

1-1. Nonlinear Proportional Gain

The proportional term considers how far the output is from the set-point at any instance in time. Its contribution to the control input depends on the product of the proportional gain and error e. As e grows or shrinks, the influence of the proportional term grows or shrinks proportionately. Therefore, the proportional gain should be properly enlarged when e is large. If a large proportional gain is maintained even for a small error when the response reaches around the set-point, excessive control may cause overshoot and oscillation. According to this fact, the proportional gain K_p(e) is given

by a set of rules in the Tagaki-Sugeno fuzzy model [23]:

$$\begin{aligned} &R^1\text{: If e is } F^1\text{, then } K_p^1(e)=a_1+a_2,\\ &R^2\text{: If e is } F^2\text{, then } K_p^2(e)=a_1,\\ &R^3\text{: If e is } F^3\text{, then } K_p^3(e)=a_1+a_2, \end{aligned} \tag{5}$$

where a_1 and a_2 are user-defined positive constants, and F^1, F^2, and F^3 are fuzzy sets with the following membership function (MF) forms:

$$F^1(x)=\begin{cases} 1, & x<-3\sigma \\ -\dfrac{1}{3\sigma}x, & -3\sigma\le x\le 0 \\ 0, & x>0 \end{cases}, \tag{6a}$$

$$F^2(x)=\exp(-x^2/2\sigma^2), \tag{6b}$$

$$F^3(x)=\begin{cases} 0, & x<0 \\ \dfrac{1}{3\sigma}x, & 0\le x\le 3\sigma \\ 1, & x>3\sigma \end{cases}, \tag{6c}$$

where σ is the standard deviation of the Gaussian function and is also a user-defined constant. Fig. 2 shows the shapes of the MFs. In this figure, F^1 represents negative, F^2 zero, and F^3 positive.

The final inferred output for $K_p(e)$ is the weighted average of the three rule outputs:

$$K_p(e)=\sum_{j=1}^{3}\rho^j K_p^j(e)/\sum_{j=1}^{3}\rho^j, \tag{7}$$

where $\rho^j=F^j(e)$. By introducing the overlap among the MFs in Fig. 2, we have the following condition:

$$\sum_{j=1}^{3}\rho^j\neq 0. \tag{8}$$

The variation of $K_p(e)$ is determined by the values of a_1 and a_2 as well as σ of the MFs. $K_p(e)$ is lower bounded by a_1 when e=0 and is upper bounded by a_1+a_2 when e=±∞. Fig. 3 illustrates the shapes of $K_p(e)$ versus e in the typical values of σ.

1-2. Nonlinear Integral Gain

The integral term addresses how long and how far the output has been away from the set-point and continuously sums up e. Thus, even a small error, if it persists, will have a sum total that grows over time, and the influence of the integral term will similarly grow.

Therefore, the integral gain $K_i(e)$ is nonlinearly adjusted depending on the size of e. That is, it is decreased to prepare for the occurrence of overshoot when e grows and enlarged to reduce the steady-state error when e shrinks. $K_i(e)$ is given as

$$\begin{aligned} &R^1\text{: If e is } F^1\text{, then } K_i^1(e)=0,\\ &R^2\text{: If e is } F^2\text{, then } K_i^2(e)=b_1,\\ &R^3\text{: If e is } F^3\text{, then } K_i^3(e)=0, \end{aligned} \tag{9}$$

where b_1 is a positive constant determined by a user, and F^1, F^2, and F^3 are the same fuzzy sets defined in Eq. (6). Fig. 4 shows the shape of $K_i(e)$ in typical values of σ. As shown in Fig. 4, $K_i(e)$ converges to the upper value b_1 when e=0 and to the lower value 0 when e=±∞.

1-3. Nonlinear Derivative Gain

The derivative term considers how fast an error changes at the current moment and increases in proportion to the product of the error rate and derivative gain. If the proportional and integral terms increase, damping is performed by predicting that the output will also enlarge; however, response can be slowed when damping is performed at more than the required level over the entire control cycle. If damping is only performed for a certain cycle, the proportional and integral terms can be utilized more drastically and overshoot can be reduced. Thus, the size of the derivative gain is changed, so that large damping can be applied when the response is in the cycle of the colored area (i.e., eė≥0), as shown in Fig. 5.

Therefore, the value of the derivative gain is changed by a set of fuzzy rules described by

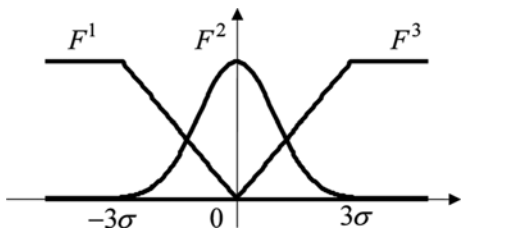

Fig. 2. Fuzzy partition over the input space.

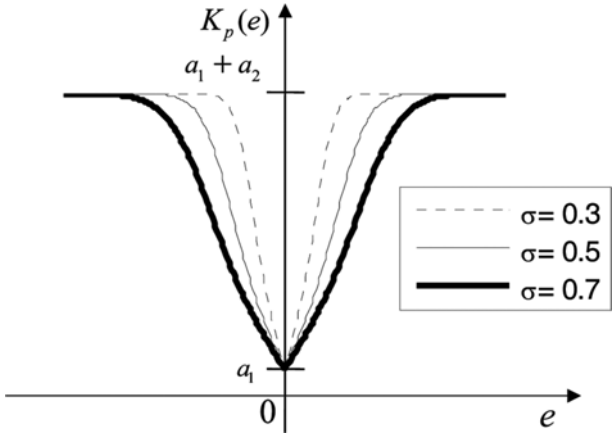

Fig. 3. Shape of $K_p(e)$ in the typical values σ.

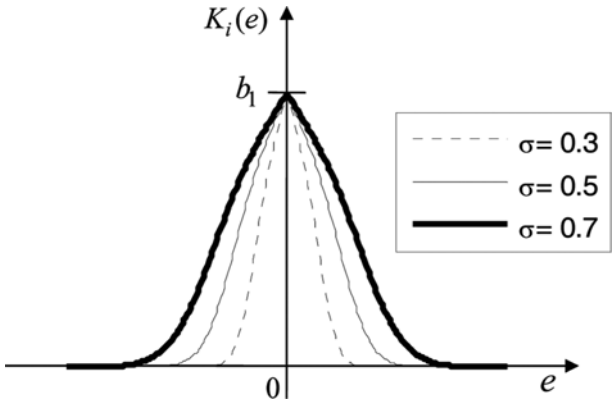

Fig. 4. Shape of $K_i(e)$ in the typical values σ.

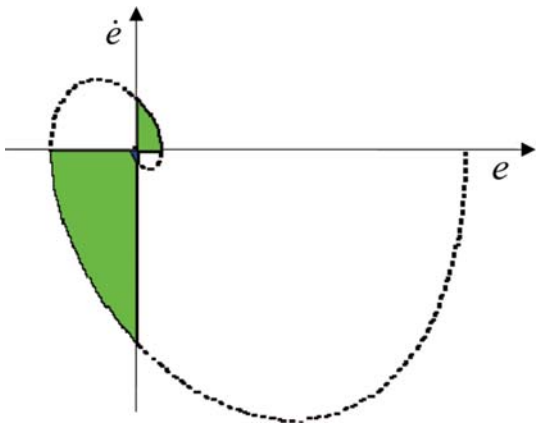

Fig. 5. e-ė phase plane.

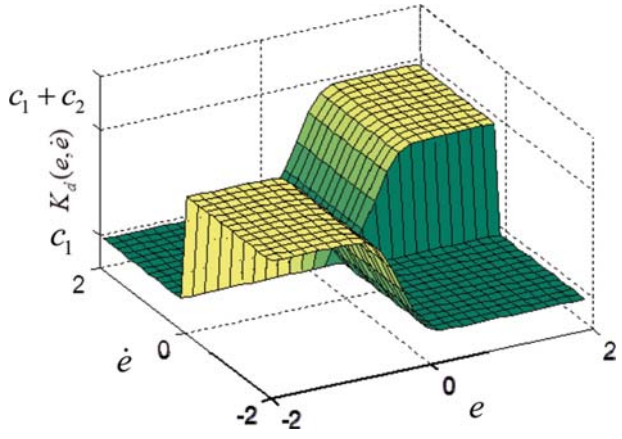

Fig. 6. Shape of K_d(e, ė) in the typical values σ=0.3.

$$\begin{aligned} &R^1\text{: If e is } F^1\text{, then } K_d^1(e,\dot{e})=c_1+c_2,\\ &R^2\text{: If e is } F^2\text{, then } K_d^2(e,\dot{e})=c_1,\\ &R^3\text{: If e is } F^3\text{, then } K_d^3(e,\dot{e})=c_1+c_2. \end{aligned} \tag{10}$$

$K_d(e, \dot{e})$ converges to $K_d(e, \dot{e})=c_1+c_2$ when $e\dot{e}\geq 0$ or $K_d(e, \dot{e})=c_1$ when $e\dot{e}<0$, where c_1 and c_2 are positive user-defined parameters. Fig. 6 shows a typical shape of $K_d(e, \dot{e})$ versus e and ė when σ=0.3.

2. Tuning of the NPID Controller

As known, the proposed NPID controller has six user-defined parameters. These parameters should be properly tuned, so that the closed-loop control system with a saturation element maintains the desired performance. The controller parameters are tuned as the following index is minimized [24]:

$$J(\boldsymbol{\phi})=\int_0^{t_f}|y_s(t)-y(t)|+\alpha|u_{sat}(t)-u_0|dt, \tag{11}$$

where y_s and y are the desired set-point and actual output, and u_{sat} and u_0 the output of the input saturation and final value of the control input, respectively. u_0 becomes zero when the CSTR remains in equilibrium. $\boldsymbol{\phi}=[a_1, a_2, b_1, c_1, c_2, \sigma]^T$ is a vector comprising the controller tuning parameters, α the weighting factor, and t_f the integral time which is sufficiently large so that the integral value after t_f can be ignored. The optimization issue is solved using a GA [25,26].

3. GA-based Gain Tuning

In this section, a set of simulation works was performed on a CSTR to compare the performance of the proposed NPID controller with those of the NPID controller proposed by Korkmaz et al. [17] (hereafter referred to as Korkmaz) and the adaptive controller proposed by Chen and Peng [4] (hereafter referred to as Chen). To maintain the fairness of comparison, the Korkmaz's NPID controller was tuned using a GA in terms of minimizing the function evaluation in Eq. (11) based on the same scenario used for the tuning of the proposed NPID controller. The parameters η=0.2, m=5, and sign(∂y/∂x)=1 were used for Chen's adaptive controller.

The principal objective of a feedback controller is typically either set-point tracking or disturbance rejection, and most of the one-degree-of-freedom PID controllers are tuned either to track a changing set-point by adjusting the process variable or to reject abrupt disturbances. In this control operation, the NPID controller for the CSTR tracks a changing set point maneuvered by a human operator in start/stop mode and continue working at a constant set-point to overcome disturbances during the normal running period.

As disturbances are especially unpredictable and the open-loop process has two stable equilibrium points, $\mathbf{x}_A=[0.144, 0.886]^T$ and $\mathbf{x}_C=[0.765, 4.705]^T$, and one unstable equilibrium point, $\mathbf{x}_B=[0.447, 2.752]^T$, under nominal values, we considered a scenario for tuning the two NPID controllers in which the system states are controlled from the first stable point $\mathbf{x}_A$ to the second unstable point $\mathbf{x}_B$ and then from the second unstable point to the third stable point $\mathbf{x}_C$. In other words, the set-point is changed with respect to t while the CSTR remains initially at $\mathbf{x}_A$; that is, y_s=2.752 for 0<t≤8, and y_s=4.705 for 8<t≤16.

D_a, γ, H and β were set to the nominal values as mentioned earlier and α set to 0.4. For the control parameters of a real-coded genetic algorithm (RCGA), P_{size}=40 for the population size, P_c=0.9 for the crossover probability, and P_m=0.05 and b=5 for the dynamic mutation are considered [25,26]. The following constraints are used in the optimization problem $0<a_1, a_2, b_1, c_1, c_2\leq 100$ and $0<\sigma\leq 3$. The tuning results of the two NPID controllers are shown in Table 1.

SIMULATION

The set-point variations are introduced for assessing the tracking performance of the proposed NPID controllers in start/stop mode. The set-point y_s is changed from 0.886 to 2.752 and from 2.752 to 4.705. Fig. 7 and Fig. 8 show the responses of the three controllers.

From the responses, all the controllers are able to track the vari-

Table 1. Tuned parameters of the proposed NPID controller and Korkmaz's NPID controller

Methods	Parameters					
	a_1	a_2	b_1	c_1	c_2	σ
Proposed	49.70	20.02	39.98	24.21	18.05	0.10
Korkmaz	33.19	42.58	15.95	1.23	13.07	-

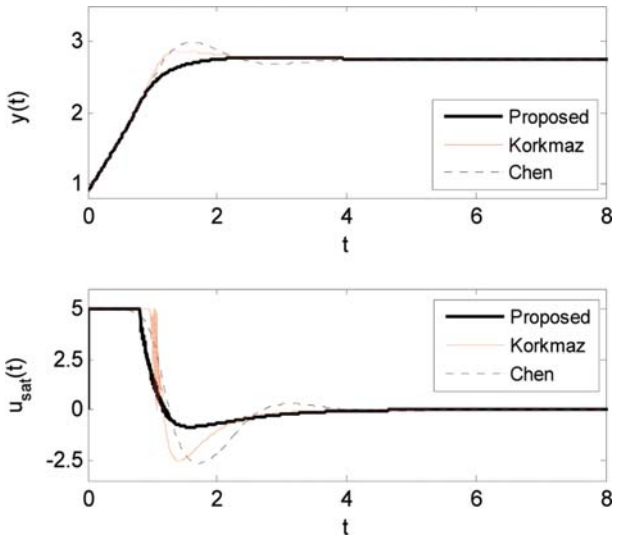

Fig. 7. Set-point tracking responses y_s=0.886→2.752.

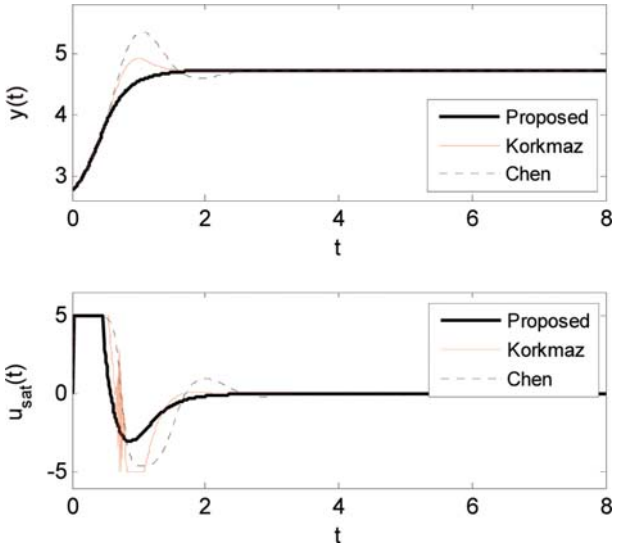

Fig. 8. Set-point tracking responses y_s=2.752→4.705.

ation in the reactor temperature without steady-state error, but the proposed NPID controller reaches faster with smaller overshoot than the other controllers. The quantitative performance measures

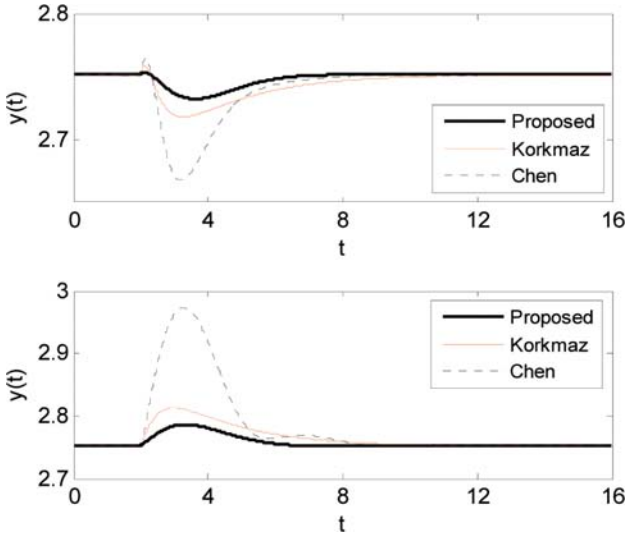

Fig. 9. Disturbance rejection responses while y_s=2.752.

like rise time ($t_r=t_{95}-t_5$), overshoot (M_p), 2% settling time (t_s) and the integral of the absolute error (IAE) are calculated as shown in Table 2. Further, it is evident that the proposed NPID controller is found to be better in all the performance measures.

Simulation work was carried out to demonstrate the disturbance rejection capability of the proposed method. Two different disturbances d_1 and d_2 are applied to the right side of Eq. (1) when the process persists at the unstable point x_B in the presence of the fixed set-point y_s=2.752. d_1=0.2 and d_2=0.2 are applied after t=2 for the first simulation of Fig. 9, and d_1=−0.2 and d_2=0.2 for the second simulation of Fig. 9. Fig. 9 demonstrates that the proposed NPID controller is able to reject the disturbance quickly and bring the output back to the nominal value of the set-point but the other methods require more time to recover from disturbances. Particularly, Chen's adaptive controller shows relatively inferior performance to the other controllers in disturbance rejection.

The performance measures, such as peak time (t_{peak}), perturbance peak (M_{peak}), and recovery time (t_{rcy}), are obtained for comparison purposes. M_{peak} indicates $|y_s-y_{max}|$ or $|y_s-y_{min}|$, and t_{rcy} is the time required for recovering the output y to less than 2% of the set-point y_s. Table 3 confirms that the proposed method and Korkmaz's NPID controller have a good overall performance. Conversely, Chen's adaptive controller shows a larger M_{peak} and a lon-

Table 2. Set-point tracking performances

Methods	y_s=0.886→2.752			
	t_r	M_p	t_s	IAE
Proposed	1.39	1.25	1.71	1.26
Korkmaz	1.02	6.12	2.47	1.27
Chen	1.06	12.74	3.39	1.37
	y_s=2.752→4.705			
Proposed	1.08	0.91	1.41	1.03
Korkmaz	0.65	10.46	1.43	0.94
Chen	0.61	32.80	2.34	1.24

Table 3. Disturbance rejection performances

Methods	d_1=0.2 and d_2=0.2			
	t_{peak}	M_{peak}	t_{rcy}	IAE
Proposed	0.71	0.05	3.63	0.09
Korkmaz	0.34	0.11	6.72	0.21
Chen	1.70	0.97	6.63	2.36
	d_1=−0.2 and d_2=0.2			
Proposed	0.78	0.05	3.97	0.10
Korkmaz	0.37	0.10	8.42	0.24
Chen	0.79	0.33	7.68	0.81

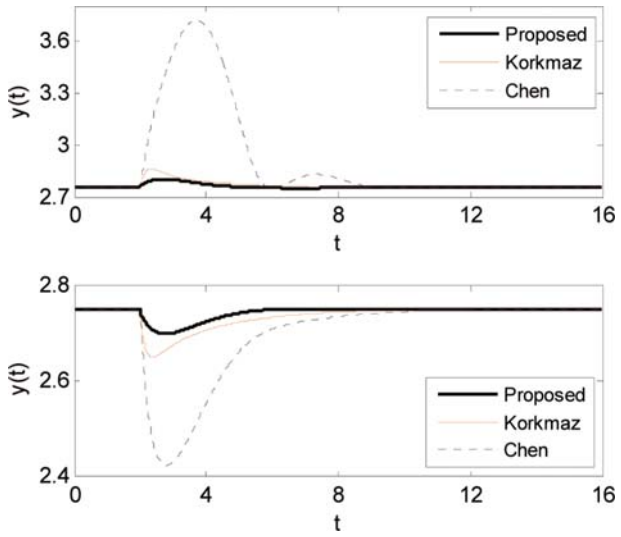

Fig. 10. Comparison of responses to parameter changes with y_s= 2.752.

ger t_{rcy} than the others.

As the CSTR is a time-varying process in which a chemical reaction takes place and may cause parameter changes during operation, two observations are obtained to examine the robustness of the proposed NPID controller by varying the CSTR parameters. The first simulation in Fig. 10 shows the results obtained while changing D_a from 0.072 to 0.09 and H from 8 to 9 simultaneously after t=2 when the control process remains at the unstable point x_B. The second simulation in Fig. 10 shows the response obtained while changing D_a from 0.072 to 0.05 and H from 8 to 7 simultaneously after t=2.

From these two simulation works, two NPID controllers were found to be less sensitive to parameter changes, but Chen's adaptive controller exhibits an unsatisfactory performance because of a larger peak value and a longer recovery time than those of the other controllers. This finding can also be confirmed in Table 4, which summarizes the quantitative results.

CONCLUSIONS

This study presented a nonlinear PID controller with a practical derivative term, a saturation element, and time-varying gains based on a standard PID frame. The proportional, integral, and derivative gains were described by a set of fuzzy rules as nonlinear functions of the error and/or error rate, and the parameters of the three gains were tuned by a GA in terms of minimizing the evaluation of the given index. This approach was applied to the temperature control of a CSTR process, and the performance was compared with that of Korkmaz's NPID controller and Chen's adaptive controller. The results indicated that the proposed controller demonstrated a better performance than the other controllers.

Although simulation studies showed that the proposed controller provided a satisfactory performance, the number of tuning parameters is 6, which may be a burden to apply in practical control problems. Therefore, as a future work, we will study the problem of reducing the number of tuning parameters.

Table 4. Parameters changing performances

Methods	D_a=0.072→0.09, H=8→9			
	t_{peak}	M_{peak}	t_{rcy}	IAE
Proposed	0.29	0.04	2.42	0.01
Korkmaz	0.30	0.09	2.48	0.07
Chen	1.71	0.97	6.64	2.36
	D_a=0.072→0.05, H=8→7			
Proposed	0.30	0.04	2.74	0.04
Korkmaz	0.32	0.08	2.86	0.08
Chen	0.80	0.33	7.69	0.81

REFERENCES

1. W. H. Ray, *Advanced Process Control*, McGraw-Hill (1981).
2. B. W. Bequette, *Process Control: Modeling, Design and Simulation*, Prentice Hall (2002).
3. C. L. Smith, *Practical Process Control: Tuning and Troubleshooting*, Wiley (2009).
4. C. T. Chen and S. T. Peng, *Int. J. Process Control*, **9**, 151 (1999).
5. W. D. Chang, *Simulation Modelling Practice Theory*, **31**, 1 (2013).
6. K. A. Dagher and A. S. Al-Araji, *Al-Khwarizmi Eng. J.*, **9**, 46 (2013).
7. M. M. Sabir and J. A. Khan, *Advances in Artificial Neural Systems*, 2014 (2014).
8. A. B. Pati, R. H. Chile and V. R. Wahane, *Michael Faraday IET Int. Summit 2015: MFIIS-2015*, 36 (2015).
9. Y. Zhuo and Q. Zhu, *2015 7th Int. Conf. on Modelling, Identification and Control* (2015).
10. T. Rasul and M. Pathak, *1st IEEE Int. Conf. on Power Electronics, Intelligent Control and Energy Systems*, 1 (2016).
11. P. Saini, S. K. Gaba, N. Rajput and A. Aggarwal, *2016 3rd Int. Conf. on Computing for Sustainable Global Development*, 2778 (2016).
12. D. A. Tamboli and R. H. Chile, *2016 Int. Conf. on Advances in Computing, Communications and Informatics*, 1410 (2016).
13. H. Seraji, *J. Robotics System*, **15**, 161 (1998).
14. Y. X. Su, D. Sun and B. Y. Duan, *Mechatronics*, **15**, 1005 (2005).
15. C. Li, S. Wang, Z. Yue, J. Yu and H. Wang, *Proc. of the 27th Chinese Conf. Control*, 377 (2008).
16. H. Zhang and B. Hu, *Proc. Int. Conf. Future Electrical Power and Energy System*, 202 (2012).
17. M. Korkmaz, O. Aydogdu and H. Dogan, *Proc. Int. Symp. Innovations in Intelligent Systems and Applications*, 1 (2012).
18. J. Chen, B. Lu, F. Fan, S. Zhu and W. Jianxin, *Appl. Mech. Mater.*, **141**, 157 (2012).
19. R. Lucas, R. M. Oliveira, C. B. Nascimento and M. S. Kaster, *2015 IEEE 24th Int. Symp. on Industrial Electronics (ISIE)*, 1022 (2015).
20. P. Mishra, V. Kumar and K. P. S. Rana, *ISA Transactions*, **58**, 434 (2015).
21. K. J. Åström and T. Hägglund, *PID Controllers: Theory, Design and Tuning*, ISA (1995).
22. A. O'Dwyer, *Handbook of PI and PID Controller Tuning Rules 3rd Ed.*, Imperial College Press (2009).
23. T. Takagi and M. Sugeno, *Fuzzy identification of systems and its*

applications to modeling and control, IEEE Trans. Syst. Man Cybern., **15**, 116 (1985).
24. R. Isermann, *Digital Control Systems*, Springer-Verlag, N. Y. (1977).
25. G. G. Jin, *Genetic Algorithms and Their Application*, Kyo-Woo Publishing Co. (2000).
26. K. Watanabe and M. M. A. Hashem, *Evolutionary Computations: New Algorithms and their Applications to Evolutionary Robots*, Springer (2004).